
This is an electronic reprint of the original article.
This reprint may differ from the original in pagination and typographic detail.

Liu, Shuman; Liu, Junguo; Zhao, Dandan; Yang, Hong

Impact of transboundary water flows on quality-induced water pressure in China

Published in:
Communications Earth and Environment

DOI:
[10.1038/s43247-025-02142-2](https://doi.org/10.1038/s43247-025-02142-2)

Published: 01/12/2025

Document Version
Publisher's PDF, also known as Version of record

Published under the following license:
CC BY-NC-ND

Please cite the original version:
Liu, S., Liu, J., Zhao, D., & Yang, H. (2025). Impact of transboundary water flows on quality-induced water pressure in China. *Communications Earth and Environment*, 6(1), Article 150. <https://doi.org/10.1038/s43247-025-02142-2>

This material is protected by copyright and other intellectual property rights, and duplication or sale of all or part of any of the repository collections is not permitted, except that material may be duplicated by you for your research use or educational purposes in electronic or print form. You must obtain permission for any other use. Electronic or print copies may not be offered, whether for sale or otherwise to anyone who is not an authorised user.

<https://doi.org/10.1038/s43247-025-02142-2>

Impact of transboundary water flows on quality-induced water pressure in China

Shuman Liu¹, Junguo Liu^{1,2}✉, Dandan Zhao^{3,4} & Hong Yang⁵

Quality-induced water pressure (P) is gaining increased attention. With the flows of transboundary water, P can be transferred among upstream and downstream regions. Here, we quantified the magnitude of pollutant transmission, and assessed its impact on individual provinces in China. On the annual basis, P was mitigated in 61% of provinces for Chemical Oxygen Demand, 87% for Ammonia Nitrogen, and 84% for Total Phosphorus, while it was intensified for 77% for Total Nitrogen in 2021. The aggregated P were mitigated in 68% of provinces, while intensified in 32% provinces. Furthermore, the monthly assessment has found that the impact of transboundary water on P varies seasonally, generally alleviating in winter and exacerbating in summer. This fluctuation was attributed to the comparatively higher quality of transboundary inflows during winter relative to local water quality. This study provides a scientific foundation for effective water management and quality control.

Water resources are essential for sustaining life, livelihoods, and production processes. Currently, about one-third of the global population is affected by water scarcity, a condition expected to deteriorate further^{1,2}. China is particularly affected by these challenges, as its per capita water resources amount to only a quarter of the global average³. This is further compounded by the uneven distribution of water resources both temporally and spatially⁴. Additionally, water pollution also exacerbates water scarcity despite great efforts in environmental water management⁵.

Water pollution adversely affects water usability, thus intensifying water scarcity^{6–8}. The emerging concept of quality-induced water scarcity has attracted great attention due to escalating pollution emissions^{9,10}. Recent studies have primarily focused on the integration of water quality factors into assessments of water scarcity^{5,11,12}. For instance, global monthly water scarcity metrics worsened when considering factors such as water temperature and other quality thresholds¹¹. In China, a comprehensive national assessment revealed that poor water quality greatly exacerbates water scarcity challenges⁵. Additionally, researchers developed an environmental sustainability index to identify water pollution hotspots across China's 31 mainland provinces¹³. Moreover, several studies have investigated the spatial and temporal variations in inland water quality and their responses to anthropogenic discharges^{14–16}.

Many studies have found that water resources and pollutants embedded in goods and services can be transferred among regions via virtual water trade, thereby redistributing quality-induced water scarcity across regions^{17–22}. In China, studies have focused particularly on regional flows. For example, a study has revealed that Shanghai, China's largest

megacity, obtains water resources from across the country and alleviates its pollution through virtual water trade¹⁷. Another study identified the primary provinces involved in outsourcing and receiving by quantifying pollution shifts in interprovincial commodity and service trade, showing that wealthier provinces play pivotal roles in pollution outsourcing, with many recipients of water pollution facing severe water quality challenges¹⁸. Moreover, investigations into the drivers of regional water scarcity, considering both quantity and quality via the blue, green, and grey water footprint, have shown that interprovincial trade intensifies water scarcity in exporting regions¹⁹. Additionally, water resources are redistributed not only through virtual water trade but also via water transfer projects. Zhao et al. compiled an inventory of both physical water transfers and virtual water flows at the provincial level, concluding that these redistributions generally alleviate water stress in China²³.

It is important to note that physical water flow also contributes to the transport of pollutants²⁴. Many researches in this field focused on employing hydraulic equations to simulate the one-, two-, and three-dimensional transport and diffusion of pollutants in water^{25,26}. These approaches rely on detailed physical, chemical, and biological parameters, making them most suitable for small-scale simulations, such as individual river sections or basins^{27,28}. With advancements in computational technology, numerous water quality models, such as SWAT, HSPF, EFDC, and DynQual, have been developed to simulate pollutant transport in various water bodies and on regional and global scale^{28–33}. Furthermore, deep learning is progressively being utilized in water quality modeling and prediction^{34–38}. These models can be calibrated using existing data to simulate periods

¹School of Environment Science and Engineering, Southern University of Science and Technology, Shenzhen, 518055, China. ²Yellow River Research Institute, North China University of Water Resources and Electric Power, Zhengzhou, 450046, China. ³Institute of Surface-Earth System Science, School of Earth System Science, Tianjin University, Tianjin, 300072, China. ⁴Water & Development Research Group, Department of Built Environment, Aalto University, PO Box 15200, 00076 Espoo, Finland. ⁵2w2e Environmental Consulting GmbH, Mettlenweg 3, Duebendorf, 8600, Switzerland. ✉e-mail: junguo.liu@gmail.com

lacking direct observations^{30,39–41}. However, they generally require intricate parameterization and are primarily designed for watershed-scale simulations^{42–46}.

Transboundary water plays a critical role in water resource management, concerning both quantity and quality^{47,48}. Although some studies have examined the impact of transboundary water flows on regional water scarcity, some research gaps remain^{49–56}. On one hand, most studies focus primarily on inter-basin water diversion projects, often overlooking natural water systems, which limits the understanding of the issue. Furthermore, these studies typically use basins as the fundamental unit of assessment, which does not align with administrative boundaries, making their findings less applicable to regional water resource management. On the other hand, research in this field has largely concentrated on the effects of transboundary water flows on water quantity, with limited attention given to their impact on water quality. In practice, these flows can either worsen or improve water quality of downstream areas, depending on whether the water they carry is of superior or inferior quality compared to local standards. Specifically, if the incoming water quality surpasses local standards, it mitigates the local pollution pressure. Conversely, if it falls below local standards, it intensifies the pressure. To address the gaps in the literature, our study will examine the transmission of both water and pollutants through physical water networks from upstream to downstream. We will quantify the impact of physical water flows on water pollution pressure at the regional administrative level. By integrating the entire water network, including water diversion projects and natural water systems, our analysis provides a more comprehensive perspective on assessing water resources and pollution pressures. With provinces serving as the primary evaluation units, the investigation aligns with administrative boundaries, facilitating regional water management. Moreover, the analysis will be based on compilation of an extensive dataset of monthly water quality monitoring records from 775 stations at transboundary points covering all the 31 provinces. This data will enable a robust analysis of pollution transfers from upstream to downstream when modeling approaches are constrained by parameter limitations. In addition, a monthly assessment will be conducted to capture intra-annual variations in transboundary pollutant transport and shifts in water pollution pressure.

Quality-induced water pressure (P), defined as the ratio of grey water footprint (GWF) to blue water resources (BWR), is a well-established indicator frequently utilized in related studies^{13,45,57–62}. Specifically, this index is appropriate for large-scale assessments, particularly in regions with comprehensive statistical data on pollutant emissions^{6,8,9,13,17}. The GWF is a key indicator of water pollution, with a larger GWF in a given region generally corresponding to higher P^{63–66}. Although the concept of the P index is not entirely novel, previous studies have primarily focused on local GWF while neglecting the influence of transboundary GWF^{6,8,9,13,64}. Notably, this study's application of the P index considers both local GWF and GWF transported from upstream. In this study, we assessed water quality using data from 775 inter-provincial monitoring stations across China (Fig. S1), calculated the transboundary loads of four selected pollutants. Then, we conducted a comprehensive assessment of quality-induced water pressure (P) in local areas alone and from the transboundary transfer of water pollutants, and investigated the impact of transboundary water flows and the accompanied pollutants on P in individual provinces. Additionally, we explored the seasonal variations of P and the impact of transboundary water flows on P throughout the year. Our findings pinpoint hotspots of P and assess both internal and external contributions for each province, providing key insights for sustainable water quality management and pollution control.

In China's water management system, Chemical Oxygen Demand (COD), Ammonia Nitrogen (NH₃-N), Total Nitrogen (TN) and Total Phosphorus (TP) are regarded as major pollutants (Table S1). Great efforts have been dedicated to monitoring and reporting these pollutants, thereby establishing a robust data foundation. Therefore, we selected these four pollutants for evaluation. We acknowledge that there are other pollutants that also affect water quality, in this nationwide study, we could not include them because of data constraints and the complexity of the characteristics

and concentration thresholds (i.e., national standards) of different pollutants, such as various heavy metals, particles, plastics, POPs, etc. To align with China's national water management objectives, we have adopted the government Environmental Quality Standards for Surface Water (GB 3838-2002), which are widely utilized in practice, as a reference for water quality standards⁶⁷.

Results and discussion

Identification of transboundary water pollution

In China, water quality is classified into five grades, with Grade I being the best and Grade V the worst. Water quality from Grades I to III is deemed suitable for human use. Therefore, grade III is commonly used as a threshold for water quality standard, beyond which water usability is reduced or even completely unusable. Analysis reveals that a large percentage of the sites experienced varying degrees of pollution exceedance in 2021 (Fig. 1). Among the pollutants, TN pollution was the most severe, followed by COD, TP, and NH₃-N. Specifically, out of 775 sites, over half recorded exceedance of TN pollution at least one month during the year. For COD, TP and NH₃-N, the exceedance rates for at least one month during the year also reached 35%, 26%, and 16%, respectively. The maximum exceedance factor is defined as the highest multiple by which inflow water quality exceeds the threshold, indicating the peak severity of pollution in transboundary water flows. For TN, COD, NH₃-N and TP, the percentages of sites with maximum exceedance factor of two or higher were 24%, 3%, 2% and 4%, respectively. Overall, transboundary water pollution in China displays a pronounced geographical gradient, with central and eastern regions experiencing higher pollution levels compared to the western regions. This pattern indicates that pollutants tend to accumulate downstream due to transboundary flows.

Furthermore, water quality of the inflow, local, and outflow varies across each province (Fig. 2). When comparing outflow to inflow, water quality deteriorated in 24, 17, 18, and 22 provinces for COD, NH₃-N, TN, and TP, respectively. The greatest changes were observed in Inner Mongolia (Fig. 2a: NM), Liaoning (Fig. 2c: LN), and Fujian (Fig. 2b, d: FJ) for COD, TN, NH₃-N and TP. The comparison between local and inflow water quality revealed that inflow tends to have better quality in 27, 25, and 22 provinces for COD, NH₃-N, TN and TP, respectively, with the largest difference in Inner Mongolia (Fig. 2a: NM), Ningxia (Fig. 2c: NX), and Shanxi (Fig. 2b, d: SX). In summary, water quality deteriorated as it flowed through in more than half of the provinces.

Quantification of transboundary water pollutants

The direction of water flow is predominantly from west to east, mirroring the national topography that slopes from the higher west to the lower east (Fig. 3a). Water transfers primarily occur in the Yangtze River basin and the coastal areas of the Pearl River basin. Provinces along the Yangtze River, including Shanghai, Jiangsu, Anhui, Hubei, Chongqing, and Sichuan, greatly contribute to transboundary water transfer (Figs. 3a and S2). In most provinces, the volume of transboundary water inflow is generally smaller than the outflow, indicating a net outflow greater than zero (Fig. 3b). Notably, Sichuan and Tibet exhibit substantially higher net outflows compared to other regions. In contrast, only Shanghai, Ningxia, and Chongqing exhibit net outflows below zero. It is noticed that provinces with large water inflow and outflow do not necessarily correspond to those with the largest net water outflows.

The load of transboundary water pollutants can be quantified through the volume of transboundary water and the associated pollutant concentrations. The transfer of pollutants mirrors the patterns of transboundary water volumes (Figs. S2 and S3). Notably, aside from several provinces along the Yangtze River (Fig. 3a), the transmission of NH₃-N from Shaanxi to Hubei also represents a large proportion (Fig. S3). There are substantial variations in transboundary pollutants across 31 provinces (Fig. 4). Most provinces exhibit a net outflow of pollutants, with Shanghai recording the highest. Theoretically, a region's pollutant outflow depends on the incoming loads, local emissions, and water bodies' self-purification

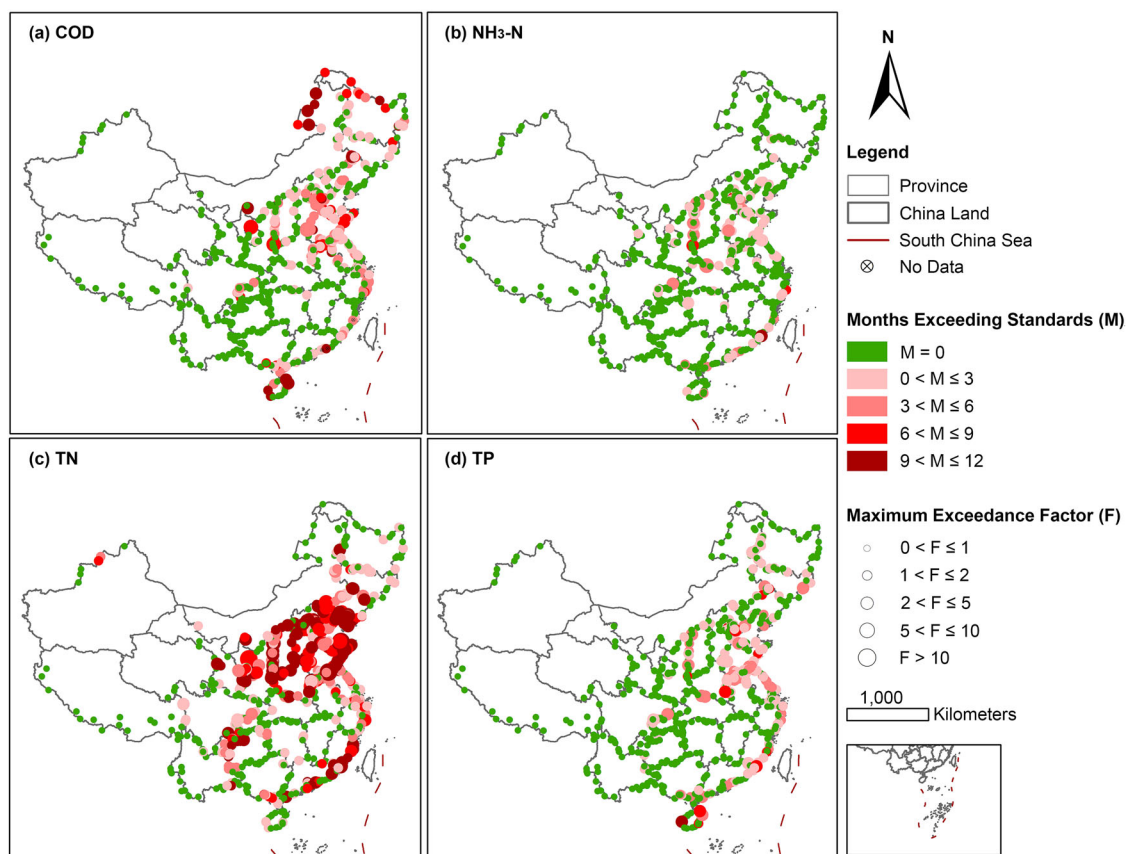


Fig. 1 | Analysis of transboundary water quality in China, 2021. a–d The result for COD, NH₃-N, TN and TP, respectively. M denotes the number of months during which water quality did not meet the established standards. F denotes the multiple by

which the peak pollution level exceeded these standards, highlighting the maximum severity of pollution in transboundary water flows from January to December. M and F are visually represented by color coding and dot size at each site, respectively.

capacities. A net outflow value below zero signifies considerable self-purification capabilities of the water bodies in the provinces.

Annual impacts on regional P

P is calculated as the ratio of GWF to blue water resources, indicating the severity of water pollution. P values of 2, 1.5, and 1 denote the thresholds for severe, moderate, and slight pressure on water resources, respectively (Fig. 5a–e). Analysis reveals that in most provinces, P values are below 1 for both the local and actual situation, implying relatively good water quality status there. It is noticed that the local P values in most provinces are higher than the actual values, implying that the quality of transboundary water inflow is better than local water quality. The water inflow actually reduced P in those recipient provinces. This situation is particularly manifested for COD, NH₃-N, and TP (Fig. 5a, b, and d). For TN, however, there are many provinces with the local P lower than the actual P, indicating inferior water quality of the inflow relative to the local water (Fig. 5c). The aggregated P, considering the GWF of dominant pollutants, shows the similar situation, with inflows reducing the actual P in 68% of the recipient provinces. Nevertheless, there are 32% provinces with actual P higher than local P, indicating the water quality of the transboundary inflow is inferior to the local water quality (Fig. 5e).

Differences between local and actual assessments result in shifts in dominant pollutants and pollution hotspots. The dominant pollutants have shifted in 12 provinces (Fig. 5f). Specifically, the predominant pollutant transitioned from TP to COD in Shanxi province, whereas in Shaanxi and Qinghai provinces, it shifted from NH₃-N to TN. In the remaining 9 provinces, such as Tianjin, Henan, and Guangdong, the dominant pollutant shifted from TP to TN. Hotspot transitions are grouped into four types, which form a basic framework for water environment management (Table S2). Notably, previously neglected hotspots like Henan and Shanxi

(Type 1) require urgent focus for developing and implementing targeted policies, infrastructure improvements, and specialized personnel. Additionally, Tianjin, Hebei, and Shandong (Type 2) also demand heightened attention, as they face not only local P challenges but also enhanced pressures from transboundary water (Table S2 and Fig. S4).

Monthly impacts on regional P

There are considerable variations in the P throughout the year (Fig. 6). A monthly assessment is conducted for the four pollutants individually and in aggregation. In general, local P is more severe during winter months than in summer months, primarily due to the low water flows in winter compared to relatively large flows in summer. This is consistent with the characteristics of the monsoon climate. The actual P is mostly lower than the local P in winter, implying better water quality in transboundary water inflow relative to the local water quality. This trend is consistent across all the four pollutants and their aggregation. Conversely, the difference between actual P and local P shows mostly positive values during the summer months, indicating that the water quality in transboundary inflows is generally worse than the local water quality during this season. This could be attributed to increased agricultural activities during the summer months, particularly fertilization applications, which lead to higher emissions of non-point source pollution in upstream areas.

It is also noticed that Ningxia (NX) has severe local P for all four pollutants. This is probably partly because of the rather small local water resources and heavy mining industries. However, the actual P is greatly reduced, mainly because of the large volume of the transboundary inflows, predominantly from the Yellow River (Fig. 6a–e). The local aggregated P is dominated by TP and COD. The actual aggregated P, however, shows a shift to TN in many provinces (Fig. 6f). This is attributable to the severe nitrogen pollution in most of transboundary water flows (Fig. S5).

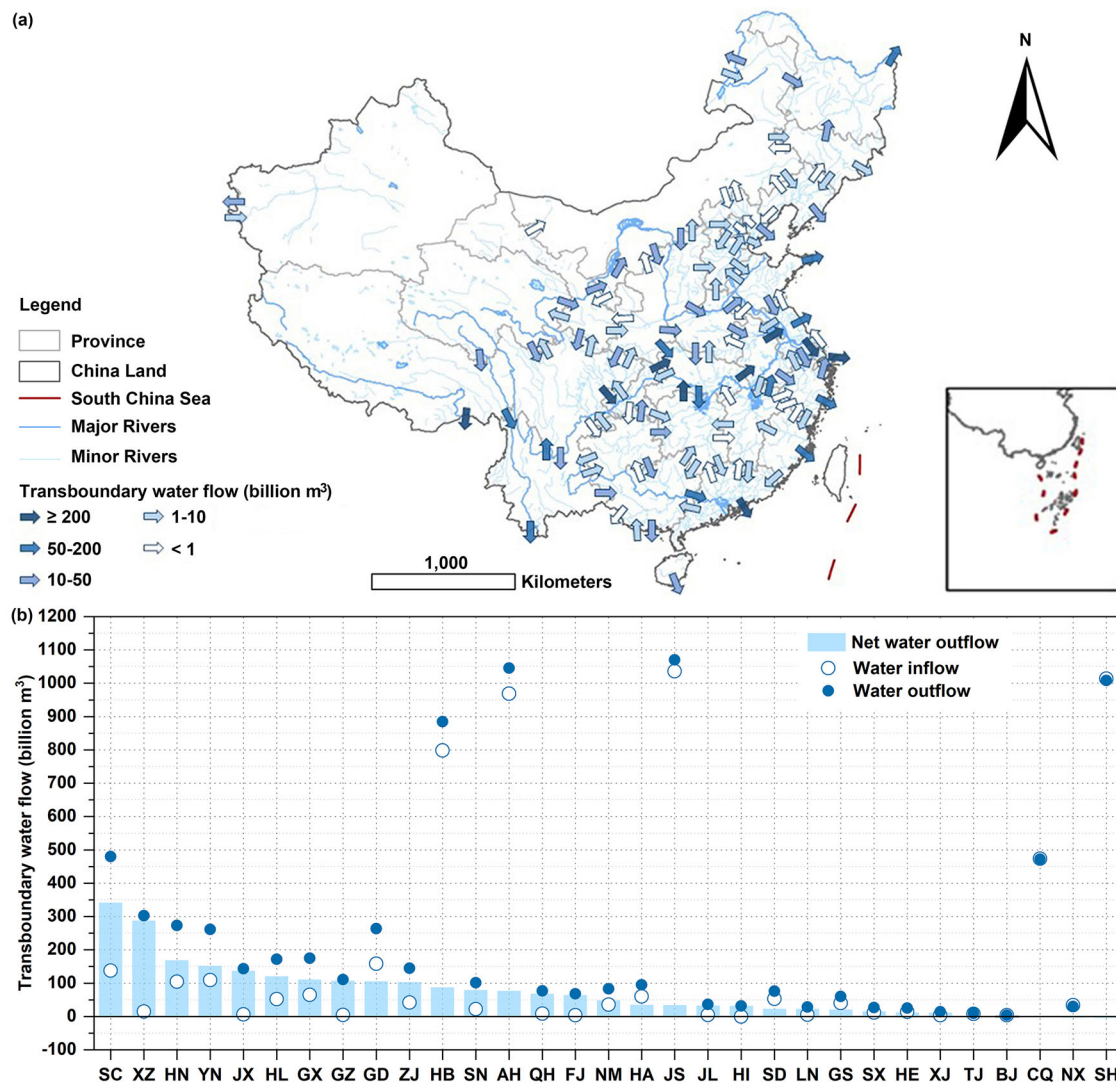


Fig. 3 | Transboundary water flows across 31 provinces. **a** The map displays arrows indicating the direction of transboundary water flows, with varying shades representing different volume ranges. **b** Statistics on transboundary water for each

province. Net outflow is depicted by column chart, while inflow and outflow are shown in scatter plots. The x-axis is organized in descending order of net outflow.

and TP in six provinces, while it is over 50% for TN in 16 provinces, constituting 19.35% and 51.61% of the total respectively. Particularly in Shanghai, external pressures contribute to more than 95% for all selected pollutants. In specific regions, available water resources primarily comprise local sources and external inflows, which can greatly influence the distribution of P (Fig. S7). In 32.26% of the provinces, external water resources are predominant. In Shanghai, external water resources account for an exceptionally high 99.47%, which substantiates the previously discussed phenomena.

Effective management of water environment necessitates addressing both local pollution and transboundary inflows. A deeper understanding of internal and external pressures provides clear insights into the primary causes of pollution, thus improving management effectiveness, particularly in P hotspots. It is essential to develop measures tailored to the unique characteristics of each region. In provinces predominantly affected by internal pressures, it is vital to strengthen the management of local pollutant sources. Conversely, in provinces facing considerable external pressures, efforts to control transboundary pollutants must be intensified. For instance, ecological restoration should be escalated in heavily polluted river sections⁶⁸. Moreover, it is essential to enhance inter-regional collaboration in pollution management, aiming to harmonize ecological conservation with economic development.

Physical and virtual water both influence water pressure

Previous studies have analyzed the virtual pollutant trade among Chinese provinces¹⁹. The results indicate that while the virtual pollutant trade exacerbates P in less developed provinces, it alleviates it in developed provinces. A comparative comparison of virtual and physical pollutant transfers highlights notable disparities in their impacts on regional P. For instance, while virtual pollutant trade intensifies P in Henan and Hebei, physical water transfer alleviates it. In contrast, P in Chongqing and Zhejiang is reduced by virtual pollutant trade but exacerbated by physical water transfer.

Recent research analyzing the impact of virtual water on the transfer of inter-provincial water pollution pressure relies on outdated data²³. Consequently, the comparative analysis between physical and virtual water trade is confined to qualitative assessments due to data inconsistencies with those used for physical pollution in our study. Future work will prioritize a quantitative analysis of the contributions of physical and virtual water to water pollution pressure, along with an exhaustive assessment of their impacts.

Limitations and future work

Quality-induced water pressure index was applied in our assessment. Although this index is a widely used indicator in related studies, it has limitations that may introduce uncertainties. Our study focuses solely on the total quantity of water and pollutants without considering the subsequent

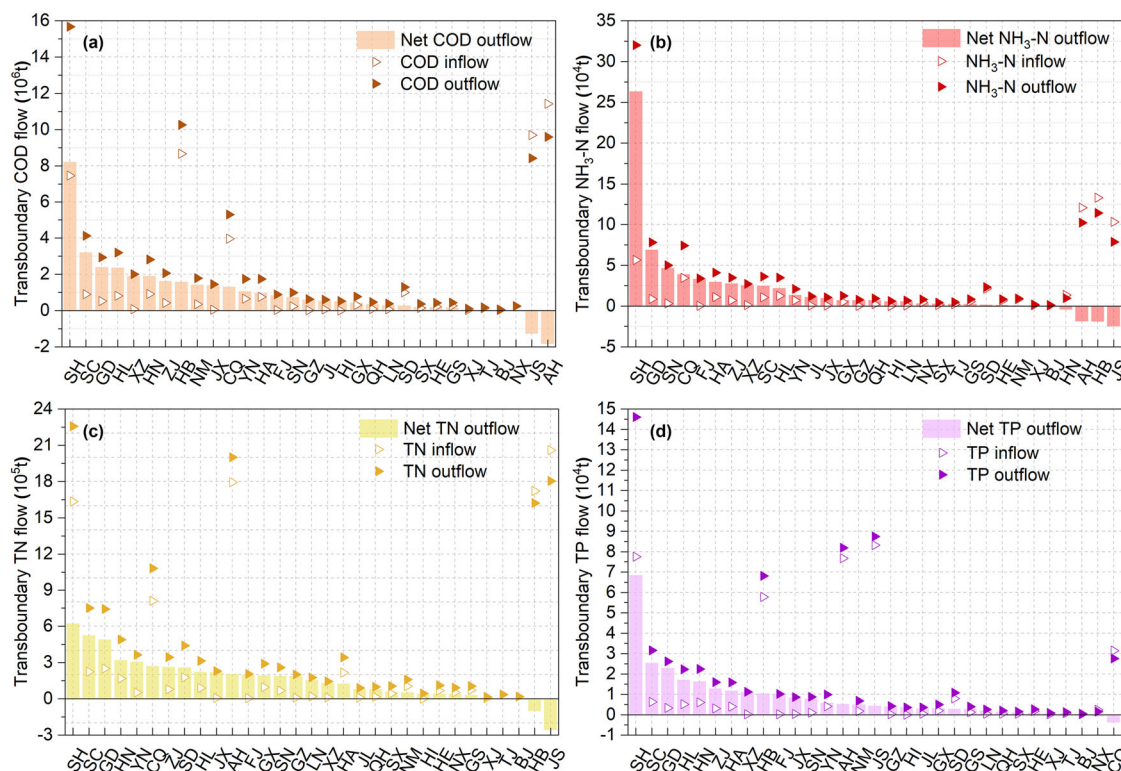


Fig. 4 | Quantification of transboundary water pollutants across 31 provinces. a–d The result for COD, NH₃-N, TN and TP, respectively. Net outflow is depicted by column chart, while inflow and outflow are shown in scatter plots. The x-axes in the subfigures are organized in descending order of net outflow.

changes that may occur after their discharge into water bodies, including complex chemical and biological processes and the various forms of pollutants in the aquatic ecosystem. In our large-scale study, accurately quantifying the specific processes that pollutants undergo upon entering water systems is challenging due to a lack of systematic reference data^{57,59}. For this reason, most studies on GWF have used specific elements as proxies for pollutant loads, regardless of the forms and fates of the pollutants, which could reduce the uncertainty introduced into the results^{59,63,64}. However, our core conclusions could be minimally impacted by this limitation for two primary reasons. On the one hand, our study examines the ‘pressure’ placed on the aquatic environment by human discharges. Consequently, the transformation of pollutants once they enter the aquatic environment is not a primary focus of our research. On the other hand, the results on P are determined by the most critical pollutants according to the GWF theory. In our study, TN was identified as the most important parameter, primarily determining the total P in the conclusions. This, to a certain extent, helps reduce the uncertainty in the conclusions.

GWF is sensitive to the selected pollutant types and the chosen water quality standards (C_{max})^{51,65,66}. Numerous water quality parameters warrant attention due to their impact on specific functions of aquatic systems. For example, nutrients can induce eutrophication in aquatic environments, resulting in algal blooms^{12,59,69}; Heavy metals present risks to both human and aquatic health^{44,46,70,71}; Salinity and water temperature are critical parameters for irrigation and power generation, respectively^{11,12,72–76}. An assessment cannot encompass all pollution types; thus, the selection of specific pollutants should be guided by the research objectives and data availability^{57,59}. In selecting the pollutants in this assessment, we initially conducted a statistical analysis of the monthly monitoring data for 20 key pollutants that are routinely monitored and publicly reported in China’s water management system (Table S1). Seven of these parameters are relatively important. Our study focuses on the four most critical pollutants (COD, NH₃-N, TN, and TP) in water bodies. The other three parameters not included in this study are water temperature, salinity and fluoride. Water temperature is generally most sensitive to atmospheric

conditions^{12,75,77–79}, resulting in exceedances that predominantly occur in summer, while the influence of transboundary water flows on downstream regions is relatively minor and difficult to discern due to the exposure in the ambient environment. Regarding salinity and fluoride, pollution levels are relatively low, and there is a lack of data on pollutant emissions. Consequently, Although the selected four key pollutants may underestimate the pollution pressure, we consider that they are sufficiently representative.

Water resources in this study considered two parts, internal water resources (refer to the total amount of water generated from local precipitation, including both surface runoff and groundwater recharge from infiltration) and transboundary water inflows. This study assesses the status quo situation of the quality-induced water pressure. We did not explicitly address the potential of interregional water transfer projects and virtual water in reducing the pressure, as they involve many complicated issues which are beyond the scope of this study.

China’s river systems are highly complex, characterized by extensive water management projects, including numerous reservoirs and both intra- and inter-basin water transfer schemes^{80–82}. This study utilizes comprehensive hydrological and water quality data from national monitoring systems to address these challenges. However, reliance on empirical data limits the scope of the study, particularly for long-term projections or applications in regions with insufficient observational data. Although models can help bridge these gaps, they require careful parameterization to ensure accuracy and are generally more suitable for basin-scale applications^{5,57,83}.

This study applied a data-driven approach in assessing the impacts of transboundary water flows on downstream regions concerning quality induced water pressure. The study is able to provide a comprehensive analysis of the status quo situation across regions in China. However, this approach has limitations in projecting the impacts under the changing circumstances. In our future work, we intend to integrate water quality models with monitoring data to support long-term and potentially global-scale studies. These will include examining in transboundary water transfers and their socio-economic impacts under various management scenarios, as

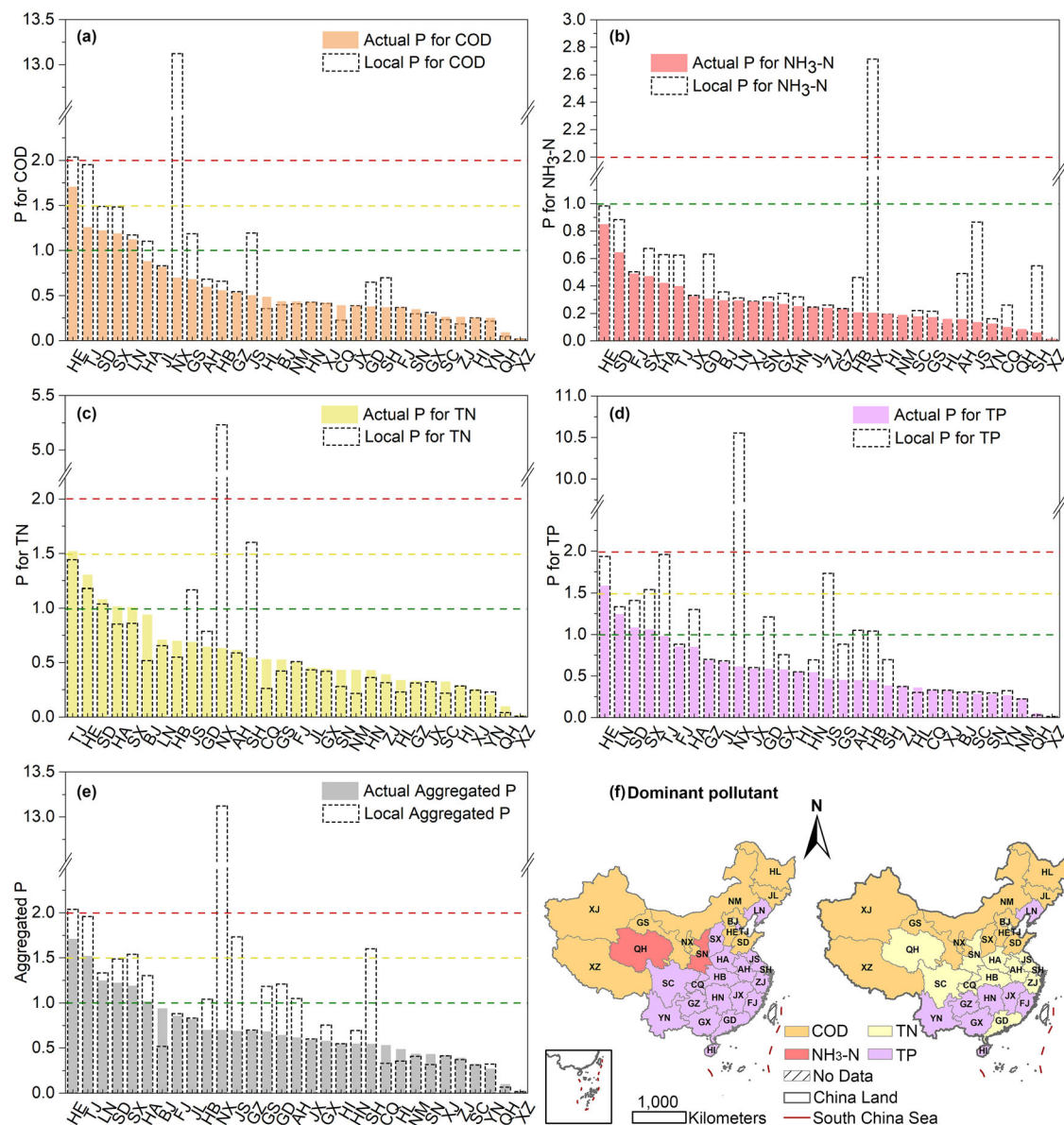


Fig. 5 | Impact of transboundary water on P for each province. a–d The result for COD, NH₃-N, TN and TP, respectively. **e** The aggregated result for these four pollutants. In **a–e** the green, yellow and red dashed lines represent thresholds for

slight, moderate, and severe P, respectively. The individual figures are arranged in descending order of actual P. **f** Identification of the dominant pollutant for local and actual aggregated P respectively.

well as incorporating the effects of climate change on transboundary water cooperation and water quality management. Such research could offer a more comprehensive understanding of the challenges and opportunities associated with transboundary water management, thereby informing the development of effective strategies for mitigating water pollution and promoting sustainable water use.

Materials and methods

Transboundary pollutants quantification

Pollutants are transported from upstream to downstream areas via transboundary water flow. Consequently, the pollution load L , can be categorized into local pollution emissions L_{local} and pollutants carried by inflow L_{inflow} .

The volumes of transported pollutants L_{inflow} were calculated as follows:

$$L_{inflow} = 0T \int Q_{inflow} * C_{act,inflow} dt = \sum_{i=1}^{12} BWR_{inflow,i} * C_{act,inflow,i} \quad (1)$$

where Q_{inflow} indicates the inflow water flux. $C_{act,inflow}$ is the weighted average of all inflow concentrations, providing a comprehensive assessment of the water quality conditions for the inflows across the region. BWR_{inflow} represents the volume of inflow water resources. The index $i = 1, 2, 3, \dots, 12$ corresponds to the months from January to December.

Quality-induced water pressure (P) assessment

Analogous to the sustainability index^{9,13,84}, the pressure index (P), derived from grey water footprint (GWF) and blue water resources (BWR). The concept suggests that if GWF exceeds the regional assimilation capacity, the GWF becomes environmentally unsustainable, potentially subjecting the region to high P^{58,59,61,62}. Specifically, 1, 1.5 and 2 are the thresholds for slight, moderate, and severe P, respectively⁹. It was quantified as follows.

$$P = \frac{GWF}{BWR} \quad (2)$$

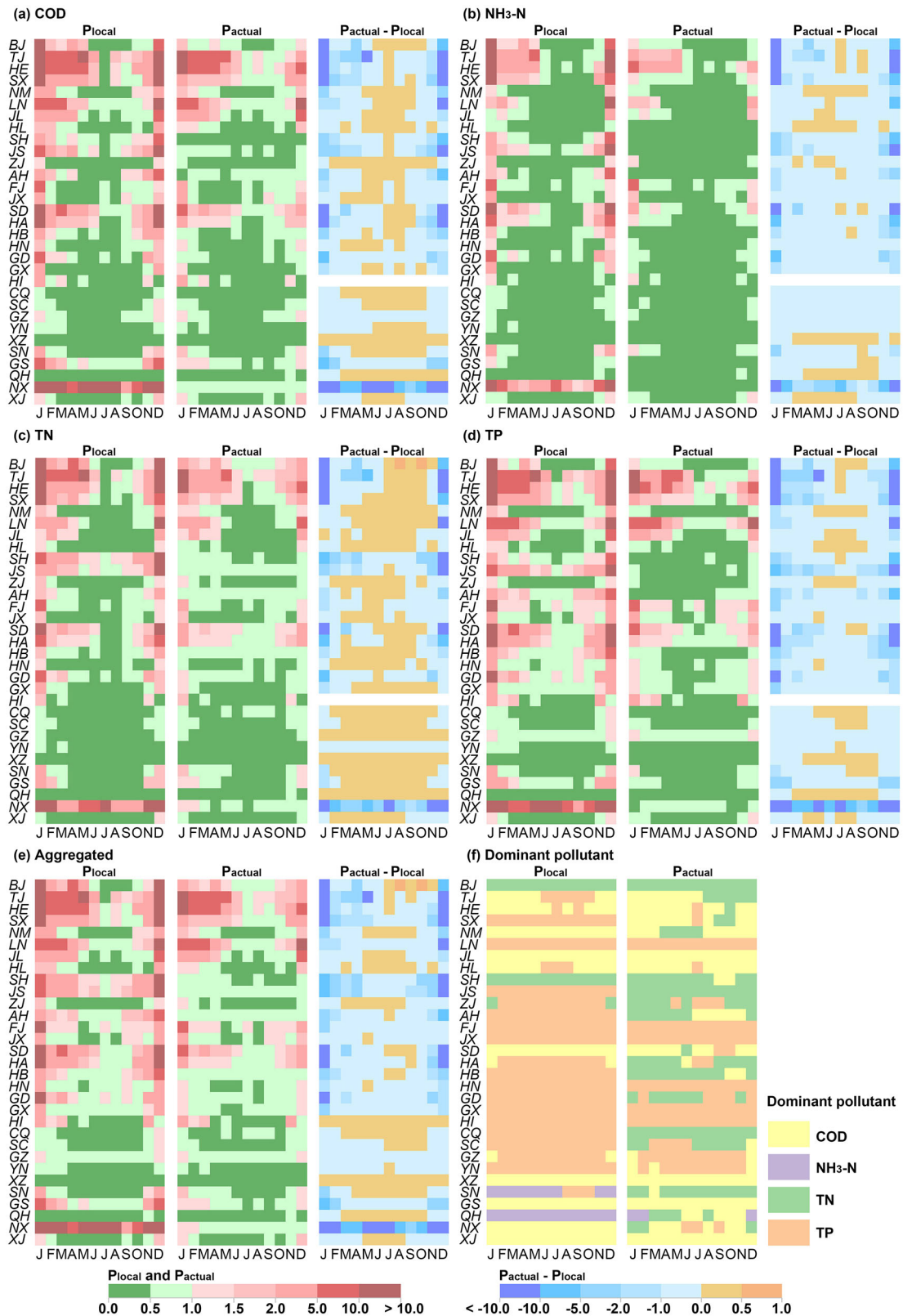


Fig. 6 | Monthly impact of transboundary water on P across province. a-d The result for COD, NH₃-N, TN, and TP respectively. e The aggregated result of the four pollutants. In a-e three graphs depict, from left to right, local P, actual P, and the

impact of transboundary water on P, respectively. The abbreviation J-D denotes the months from January to December. f Identification of the dominant pollutant for local and actual aggregated P respectively.

Thereinto, GWF is defined as the volume of freshwater that is required to assimilate the load of pollutants based on the ambient water quality standards and natural background concentrations⁶¹. It can effectively reflect the intensity of water pollution resulting from human water use activities^{45,57,59}. The calculation was as follows:

$$GWF = \frac{L}{C_{max} - C_{nat}} \quad (3)$$

where L indicates the load of water pollutants; C_{max} denotes the maximum permissible concentration as dictated by ambient water quality standards; and C_{nat} refers to the natural concentration in the receiving water body without any human disturbance.

Local pressure. Local pressure arises when the transmission of water and pollutants is overlooked, resulting in local water resources bearing the burden of local pollutants.

The local pressure was calculated as follows:

$$P_{local} = \frac{GWF_{local}}{BWR_{local}} \quad (4)$$

where GWF_{local} and BWR_{local} indicates the local grey water footprint and blue water resources, respectively.

Actual pressure. The actual P considers both pollutants and water transmission from upstream sources. This indicates that the combined total of local and incoming water resources is responsible for carrying pollutants from both local and upstream sources.

The actual pressure was calculated as follows:

$$P_{actual} = \frac{GWF_{local} + GWF_{inflow}}{BWR_{local} + BWR_{inflow}} \quad (5)$$

where GWF_{inflow} and BWR_{inflow} represent the incoming grey water footprint and blue water resources from upstream areas, respectively.

Comprehensive pressure. Based on the concept of GWF, the comprehensive pressure index should be identified as the maximum values of these four pollutants^{13,61}.

$$P_{comprehensive} = MAX\{P_{COD}, P_{NH_3-N}, P_{TN}, P_{TP}\} \quad (6)$$

Impact of transboundary water on regional P. Consequently, the impact of transboundary water on regional P can be quantified by the corresponding increase in parameter P as follows:

$$P^* = P_{actual} - P_{local} \quad (7)$$

For more details on the method, please refer to the Step-by-Step Guidance on Data Processing and Analysis in the Supplementary Material.

Monthly assessment

In specific water usage sectors, increased consumption directly correlates with heightened pollutant emissions¹⁸. Consequently, we adopted a method to distribute the annual pollutant load monthly, adjusting it in proportion to monthly water usage⁵. The pollutant loads from industrial, agricultural (including crop cultivation and animal husbandry), and domestic sectors were each allocated to monthly data separately. We assumed that pollution from the industrial and animal husbandry sectors was uniformly distributed throughout the year^{5,85}. Pollution from crop cultivation was adjusted monthly based on precipitation levels, reflecting the dynamics of non-point source pollution⁸⁵. Additionally, we introduced a temperature-dependent monthly factor for domestic water use to account for seasonal variations, as demonstrated in previous studies^{5,86,87}.

Local BWR primarily originate from rainfall. Consequently, the monthly BWR estimates were derived from the within-year distribution of precipitation.

Data sources

C_{max} and C_{nat} are parameters shared by both GWF_{local} and GWF_{inflow} . Previous literature did not provide specific values for C_{nat} across province. It was generally assumed to be 0 for the four pollutants in previous studies, and we followed this value^{4,6,13,61}. According to the Environmental Quality Standards for Surface Water of China⁶⁷, Grade III water is deemed suitable for most human activities, with lower grades adversely affecting water body functions. Consistent with prior research, Grade III has been adopted as the ambient water quality standard in this study. Consequently, the C_{max} for COD, NH_3-N and TP have been set as $20 \text{ mg}\cdot\text{L}^{-1}$, $1 \text{ mg}\cdot\text{L}^{-1}$ and $0.2 \text{ mg}\cdot\text{L}^{-1}$, respectively^{4,6,9}. Although TN is not explicitly mentioned in the referenced standards for rivers, recent literature highlights the importance of managing nitrogen pollution, with several studies recommending a TN standard of $3 \text{ mg}\cdot\text{L}^{-1}$ ^{58,59}.

Additionally, L_{local} and L_{inflow} are essential for GWF_{local} and GWF_{inflow} , respectively. The emission load L_{local} for each pollutant across 31 mainland provinces was sourced from the China Statistical Yearbook⁸⁸. L_{inflow} was derived from BWR_{inflow} and $C_{act, inflow}$. The majority of the annual BWR_{inflow} for 31 provinces were obtained from the Water Resources Bulletin of China and individual provincial reports⁸⁹, which was similarly the case for BWR_{local} . In regions lacking statistical data, estimations were made using measured flow data or the average annual natural runoff over multiple years⁹⁰. The monthly transboundary water volume was estimated based on the annual water volume and the intra-annual distribution patterns observed at control stations within the relevant basin. Further details are available in Table S3 and Fig. S8. Monthly water quality monitoring data for transboundary stations in 2021 were obtained from the official website of China's national surface water quality monitoring system⁹¹.

Temperature and precipitation data for each month were essential for downscaling to monthly levels, utilizing ERA5-Land datasets (<https://cds.climate.copernicus.eu>).

Reporting summary

Further information on research design is available in the Nature Portfolio Reporting Summary linked to this article.

Data availability

All data are available on Zenodo (<https://zenodo.org/records/14873532>).

Received: 25 July 2024; Accepted: 17 February 2025;

Published online: 26 February 2025

References

1. He, C. et al. Future global urban water scarcity and potential solutions. *Nat. Commun.* **12**, 1–11 (2021).
2. Naddaf, M. The world faces a water crisis — 4 powerful charts show how. *Nature* **615**, 774–775 (2023).
3. Zhang, Z. et al. City-level water withdrawal in China: Accounting methodology and applications. *J. Indus. Ecol.* 1–14 <https://doi.org/10.1111/jiec.12999> (2020)
4. Liu, J. et al. Water scarcity assessments in the past, present, and future. *Earth's Future* **5**, 545–559 (2017).
5. Ma, T. et al. Pollution exacerbates China's water scarcity and its regional inequality. *Nat. Commun.* **11**, 1–9 (2020).
6. Liu, J., Liu, Q. & Yang, H. Assessing water scarcity by simultaneously considering environmental flow requirements, water quantity, and water quality. *Ecol. Indic.* **60**, 434–441 (2016).
7. Veldkamp, T. I. E. et al. Water scarcity hotspots travel downstream due to human interventions in the 20th and 21st century. *Nat. Commun.* **8**, 15697 (2017).

8. Zeng, Z., Liu, J. & Savenije, H. H. G. A simple approach to assess water scarcity integrating water quantity and quality. *Ecol. Indicat.* **34**, 441–449 (2013).
9. Liu, J. & Zhao, D. Three-dimensional water scarcity assessment by considering water quantity, water quality, and environmental flow requirements: Review and prospect. *Kexue Tongbao/Chinese Science Bulletin* **65**, 4251–4261 (2020).
10. Boretti, A. & Rosa, L. Reassessing the projections of the World Water Development Report. *npj Clean Water* **2**, 15 (2019).
11. Van Vliet, M. T. H., Florke, M. & Wada, Y. Quality matters for water scarcity. *Nat. Geosci.* **10**, 800–802 (2017).
12. van Vliet, M. T. H. et al. Global water scarcity including surface water quality and expansions of clean water technologies. *Environ. Res. Lett.* **16**, 024020 (2021).
13. Liu, J. et al. Environmental Sustainability of Water Footprint in Mainland China. *Geograph. Sustain.* **1**, 8–17 (2020).
14. Ma, T. et al. China's improving inland surface water quality since 2003. *Sci. Adv.* **6**, eaau3798 (2020).
15. Li, Y. et al. Urbanization and agriculture intensification jointly enlarge the spatial inequality of river water quality. *Sci. Total Environ.* **878**, 162559 (2023).
16. Ezzati, G., Kyllmar, K. & Barron, J. Long-term water quality monitoring in agricultural catchments in Sweden: Impact of climatic drivers on diffuse nutrient loads. *Sci. Total Environ.* **864**, 160978 (2022).
17. Zhao, X. et al. Burden shifting of water quantity and quality stress from megacity Shanghai. *Water Resour. Res.* **52**, 6916–6927 (2016).
18. Wu, Z. & Ye, Q. Water pollution loads and shifting within China's inter-province trade. *J. Clean. Product.* **259**, 120879 (2020).
19. Cai, B. & Guo, M. Exploring the drivers of quantity- and quality-related water scarcity due to trade for each province in China. *J. Environ. Manag.* **333**, 117423 (2023).
20. Garcia, S., Rushforth, R., Ruddell, B. L. & Mejia, A. Full Domestic Supply Chains of Blue Virtual Water Flows Estimated for Major U.S. Cities. *Water Resour. Res.* **56**, 1–20 (2020).
21. Chini, C. M., Djehdian, L. A., Lubega, W. N. & Stillwell, A. S. Virtual water transfers of the US electric grid. *Nat. Energ.* **3**, 1115–1123 (2018).
22. Salmoral, G. & Yan, X. Food-energy-water nexus: A life cycle analysis on virtual water and embodied energy in food consumption in the Tamar catchment, UK. *Resources. Conserv. Recycl.* **133**, 320–330 (2018).
23. Zhao, X. et al. Physical and virtual water transfers for regional water stress alleviation in China. *Proc. Natl Acad. Sci. USA* **112**, 1031–1035 (2015).
24. Mitsch, W. J. Environmental modeling: Fate and transport of pollutants in water, air, and soil. *J. Environ. Qual.* **26**, 1192 (1997).
25. Chapra, S. C. *Surface water-quality modeling*. (Waveland press, 2008).
26. Fischer, H. B., List, J. E., Koh, C. R., Imberger, J. & Brooks, N. H. *Mixing in inland and coastal waters*. (Elsevier, 2013).
27. Okubo, A. & Levin, S. A. *Diffusion and ecological problems: modern perspectives*. vol. 14 (Springer, 2001).
28. Li, Y., Shi, Y., Jiang, L., Zhu, X. & Gong, R. Advances in surface water environment numerical models. *Water Resour. Protect.* **35**, 1–8 (2019).
29. Jones, E. R. et al. DynQual v1.0: a high-resolution global surface water quality model. *Geosci. Model Dev.* **16**, 4481–4500 (2023).
30. Jones, E. R., Bierkens, M. F. P. & Van Vliet, M. T. H. *Past and future global surface water quality modelling using DynQual*. 4–5 (2024)
31. van Vliet, M. T. H., Franssen, W. H. P. & Yearsley, J. R. Global modelling of river water quality under climate change. *Geophys. Res. Abstract. EGU Gen. Assem. 2017* **19**, EGU2017–EGU4713 (2017).
32. van Vliet, M. T. et al. Model inter-comparison design for large-scale water quality models. *Curr. Opin. Environ. Sustain.* **36**, 59–67 (2019).
33. Chen, X. et al. In-stream surface water quality in China: A spatially-explicit modelling approach for nutrients. *J. Clean. Product.* **334**, 130208 (2022).
34. Desbureaux, S. et al. Mapping global hotspots and trends of water quality (1992–2010): a data driven approach. *Environ. Res. Lett.* **17**, 114048 (2022).
35. Huang, S., Wang, Y. & Xia, J. Which riverine water quality parameters can be predicted by meteorologically-driven deep learning? *Sci. Total Environ.* **946**, 174357 (2024).
36. Huang, S., Xia, J., Wang, Y., Lei, J. & Wang, G. Water quality prediction based on sparse dataset using enhanced machine learning. *Environ. Sci. Ecotechnol.* **20**, 100402 (2024).
37. Huang, S. et al. Pollution loads in the middle-lower Yangtze river by coupling water quality models with machine learning. *Water Res.* **263**, 122191 (2024).
38. Tiyasha, Tung, T. M. & Yaseen, Z. M. A survey on river water quality modelling using artificial intelligence models: 2000–2020. *J. Hydrol.* **585**, 124670 (2020).
39. Baccour, S. et al. Water quality management could halve future water scarcity cost-effectively in the Pearl River Basin. *Nat. Commun.* **15**, 5669 (2024).
40. Wang, M. et al. A triple increase in global river basins with water scarcity due to future pollution. *Nat. Commun.* **15**, 1–13 (2024).
41. Jones, E. R., Bierkens, M. F. P. & van Vliet, M. T. H. Current and future global water scarcity intensifies when accounting for surface water quality. *Nat. Clim. Chang.* **14**, 629–635 (2024).
42. Cho, K. H., Pachepsky, Y., Ligaray, M., Kwon, Y. & Kim, K. H. Data assimilation in surface water quality modeling: A review. *Water Res.* **186**, 116307 (2020).
43. Stokal, M. et al. Global multi-pollutant modelling of water quality: scientific challenges and future directions. *Curr. Opin. Environ. Sustain.* **36**, 116–125 (2019).
44. Zhou, L. et al. Model-based evaluation of reduction strategies for point and nonpoint source Cd pollution in a large river system. *J. Hydrol.* **622**, 129701 (2023).
45. Zuo, D. et al. The response of non-point source pollution to land use change and risk assessment based on model simulation and grey water footprint theory in an agricultural river basin of Yangtze River, China. *Ecol. Indicat.* **154**, 110581 (2023).
46. Zhou, L. et al. Modeling transport and fate of heavy metals at the watershed scale: State-of-the-art and future directions. *Sci. Total Environ.* **878**, 163087 (2023).
47. Feitelson, E. The Upcoming Challenge: Transboundary Management of the Hydraulic Cycle. *Water, Air, and Soil Pollution*. <https://doi.org/10.1023/A:1005269001462>. (2000)
48. Jager, N. W. Transboundary Cooperation in European Water Governance – A set-theoretic analysis of International River Basins. *Environ. Policy Govern.* **26**, 278–291 (2016).
49. Dobbs, G. R. et al. Inter-basin surface water transfers database for public water supplies in conterminous United States, 1986–2015. *Sci. Data* **10**, 1–12 (2023).
50. Sun, S. et al. Water transfer infrastructure buffers water scarcity risks to supply chains. *Water Res.* **229**, 119442 (2023).
51. Liu, J. et al. Water conservancy projects in China: Achievements, challenges and way forward. *Glob. Environ. Chang.* **23**, 633–643 (2013).
52. Kattel, G. R., Shang, W., Wang, Z. & Langford, J. China's South-to-North Water Diversion Project empowers sustainable water resources system in the north. *Sustainability (Switzerland)* **11**, 3735 (2019).
53. Munia, H. A. et al. Future Transboundary Water Stress and Its Drivers Under Climate Change: A Global Study. *Earth's Future* **8**, 1–21 (2020).
54. Duan, K. et al. Evolving efficiency of inter-basin water transfers in regional water stress alleviation. *Resour. Conserv. Recycl.* **191**, 106878 (2023).

55. Liu, H., Yin, J. & Feng, L. The Dynamic Changes in the Storage of the Danjiangkou Reservoir and the Influence of the South-North Water Transfer Project. *Sci. Rep.* **8**, 8710 (2018).
56. Barnett, J., Rogers, S., Webber, M., Finlayson, B. & Wang, M. Sustainability: Transfer project cannot meet China's water needs. *Nature* **527**, 295–297 (2015).
57. Jamshidi, S., Imani, S. & Delavar, M. An approach to quantifying the grey water footprint of agricultural productions in basins with impaired environment. *J. Hydrol.* **606**, 127458 (2022).
58. D'Ambrosio, E., De Girolamo, A. M. & Rulli, M. C. Assessing sustainability of agriculture through water footprint analysis and in-stream monitoring activities. *J. Clean. Product.* **200**, 454–470 (2018).
59. Liu, W., Antonelli, M., Liu, X. & Yang, H. Towards improvement of grey water footprint assessment: With an illustration for global maize cultivation. *J. Clean. Product.* **147**, 1–9 (2017).
60. Pellicer-Martínez, F. & Martínez-Paz, J. M. The Water Footprint as an indicator of environmental sustainability in water use at the river basin level. *Sci. Total Environ.* **571**, 561–574 (2016).
61. Hoekstra, A. Y., Chapagain, A. K., Aldaya, M. M. & Mekonnen, M. M. *The Water Footprint Assessment Manual. Setting the Global Standard.* vol. 31 (Earthscan Press, 2011).
62. D'Ambrosio, E., Gentile, F. & De Girolamo, A. M. Assessing the sustainability in water use at the basin scale through water footprint indicators. *J. Clean. Product.* **244**, 118847 (2020).
63. Hoekstra, A. Y. & Mekonnen, M. M. The water footprint of humanity. *Proc. Natl Acad. Sci. USA* **109**, 3232–3237 (2012).
64. Mekonnen, M. M. & Hoekstra, A. Y. Global Gray Water Footprint and Water Pollution Levels Related to Anthropogenic Nitrogen Loads to Fresh Water. *Environ. Sci. Technol.* **49**, 12860–12868 (2015).
65. Zhuo, L., Mekonnen, M. M., Hoekstra, A. Y. & Wada, Y. Inter- and intra-annual variation of water footprint of crops and blue water scarcity in the Yellow River basin (1961–2009). *Adv. Water Resour.* **87**, 29–41 (2016).
66. Gil, R., Bojacá, C. R. & Schrevens, E. Uncertainty of the Agricultural Grey Water Footprint Based on High Resolution Primary Data. *Water Resour. Manag.* **31**, 3389–3400 (2017).
67. Ministry of Ecology and Environment of the People's Republic of China. Environmental Quality Standards for Surface Water of China. (2003).
68. Liu, J., Cui, W., Tian, Z. & Jia, J. Theory of stepwise ecological restoration. *Kexue Tongbao/Chinese Science Bulletin* **66**, 1014–1025 (2021).
69. Suresh, K. et al. Recent advancement in water quality indicators for eutrophication in global freshwater lakes. *Environ. Res. Lett.* **18**, 063004 (2023).
70. Zheng, B., Huang, G., Liu, L., Zhai, M. & Li, Y. Two-pathway perspective for heavy metal emission mitigation: A case study of Guangdong Province, China. *Sci. Total Environ.* **735**, 139583 (2020).
71. Wu, H. et al. Evaluating surface water quality using water quality index in Beiyun River, China. *Environ. Sci. Pollut. Res.* **27**, 35449–35458 (2020).
72. Thorslund, J., Bierkens, M. F. P., Scaini, A., Sutanudjaja, E. H. & Van Vliet, M. T. H. Salinity impacts on irrigation water-scarcity in food bowl regions of the US and Australia. *Environ. Res. Lett.* **17**, 084002 (2022).
73. Flörke, M., Bärlund, I., van Vliet, M. T., Bouwman, A. F. & Wada, Y. Analysing trade-offs between SDGs related to water quality using salinity as a marker. *Curr. Opin. Environ. Sustain.* **36**, 96–104 (2019).
74. Jones, E. & van Vliet, M. T. H. Drought impacts on river salinity in the southern US: Implications for water scarcity. *Sci. Total Environ.* **644**, 844–853 (2018).
75. Van Vliet, M. T. H., Wiberg, D., Leduc, S. & Riahi, K. Power-generation system vulnerability and adaptation to changes in climate and water resources. *Nat. Clim. Chang.* **6**, 375–380 (2016).
76. van Vliet, M. T. H. et al. Multi-model assessment of global hydropower and cooling water discharge potential under climate change. *Glob. Environ. Chang.* **40**, 156–170 (2016).
77. Van Vliet, M. T. H. et al. Global river discharge and water temperature under climate change. *Glob. Environ. Chang.* **23**, 450–464 (2013).
78. van Vliet, M. T. H. et al. Global river water quality under climate change and hydroclimatic extremes. *Nat. Rev. Earth Environ.* **4**, 687–702 (2023).
79. Whitehead, P. G., Wilby, R. L., Battarbee, R. W., Kernan, M. & Wade, A. J. A review of the potential impacts of climate change on surface water quality. *Hydrol. Sci. J.* **54**, 101–121 (2009).
80. Liu, J., Zhao, D., Gerbens-Leenes, P. W. & Guan, D. China's rising hydropower demand challenges water sector. *Sci. Rep.* **5**, 1–14 (2015).
81. Veldkamp, T. I. E. et al. Changing mechanism of global water scarcity events: Impacts of socioeconomic changes and inter-annual hydro-climatic variability. *Glob. Environ. Chang.* **32**, 18–29 (2015).
82. Vanham, D. et al. Physical water scarcity metrics for monitoring progress towards SDG target 6.4: An evaluation of indicator 6.4.2 "Level of water stress. *Sci. Total Environ.* **613–614**, 218–232 (2018).
83. Jamshidi, S., Imani, S. & Delavar, M. Impact Assessment of Best Management Practices (BMPs) on the Water Footprint of Agricultural Productions. *Int. J. Environ. Res.* **14**, 641–652 (2020).
84. Liu, C., Kroeze, C., Hoekstra, A. Y. & Gerbens-Leenes, W. Past and future trends in grey water footprints of anthropogenic nitrogen and phosphorus inputs to major world rivers. *Ecol. Indicat.* **18**, 42–49 (2012).
85. He, B. & Hu, M. Evaluation of agriculture non-point pollution load and its characteristics in all districts and counties of Guangdong. *Ecol. Environ. Sci.* **31**, 771–776 (2022).
86. Wada, Y. et al. Global monthly water stress: 2. Water demand and severity of water stress. *Water Resour. Res.* **47**, 1–17 (2011).
87. Voisin, N. et al. One-Way coupling of an integrated assessment model and a water resources model: Evaluation and implications of future changes over the US Midwest. *Hydrol. Earth Syst. Sci.* **17**, 4555–4575 (2013).
88. National Bureau of Statistics and Ministry of Ecology and Environment of the People's Republic of China, China Statistical Yearbooks on Environmental. (2021).
89. Ministry of Water Resources of the People's Republic of China, Water resource bulletin. (2021). Available at: <http://www.mwr.gov.cn>
90. Linke, S. et al. Global hydro-environmental sub-basin and river reach characteristics at high spatial resolution. *Sci. Data* **6**, 1–15 (2019).
91. Ministry of Ecology and Environment of the People's Republic of China, National surface water quality automatic monitoring system. (2021). Available at: <https://www.mee.gov.cn>

Acknowledgements

This study was supported by the 111 Project (Grant No. D25014), the National Foreign Experts Program (Category S) (Grant No. S20240116), Henan Provincial Key Laboratory of Hydrosphere and Watershed Water Security, the Henan Province Foreign Scientist Studio for Synergistic Management of Water, Food, Energy, and Carbon (Grant No. GZS2024013), and National Natural Science Foundation of China (Grant No. 42401379). This work was performed as part of the IAHS HELPING Working Group on Stepwise Ecological Restoration of Watersheds and on Acceptance of Nature-based Solutions & Their Implementation in Guidelines.

Author contributions

S.L. conceived the original idea, which was further developed in collaboration with J.L., H.Y., and D.Z. S.L. conducted data collection and analysis, then drafted the initial version of the manuscript. J.L., H.Y., and D.Z. contributed to result interpretation, discussion, and manuscript refinement. J.L. supervised the project.

Competing interests

The authors declare no competing interests.

Additional information

Supplementary information The online version contains supplementary material available at <https://doi.org/10.1038/s43247-025-02142-2>.

Correspondence and requests for materials should be addressed to Junguo Liu.

Peer review information *Communications Earth and Environment* thanks the anonymous reviewers for their contribution to the peer review of this work. Primary Handling Editors: Somaparna Ghosh [A peer review file is available].

Reprints and permissions information is available at <http://www.nature.com/reprints>

Publisher's note Springer Nature remains neutral with regard to jurisdictional claims in published maps and institutional affiliations.

Open Access This article is licensed under a Creative Commons Attribution-NonCommercial-NoDerivatives 4.0 International License, which permits any non-commercial use, sharing, distribution and reproduction in any medium or format, as long as you give appropriate credit to the original author(s) and the source, provide a link to the Creative Commons licence, and indicate if you modified the licensed material. You do not have permission under this licence to share adapted material derived from this article or parts of it. The images or other third party material in this article are included in the article's Creative Commons licence, unless indicated otherwise in a credit line to the material. If material is not included in the article's Creative Commons licence and your intended use is not permitted by statutory regulation or exceeds the permitted use, you will need to obtain permission directly from the copyright holder. To view a copy of this licence, visit <http://creativecommons.org/licenses/by-nc-nd/4.0/>.

© The Author(s) 2025